2-D THERMOELASTIC ANALYSIS OF LMFBR FUEL ROD CLADDINGS

L. WOLF, Ch. N. WONG, M. K. YEUNG

Department of Nuclear Engineering,
Massachusetts Institute of Technology, Cambridge, Massachusetts 02139, U.S.A.

SUMMARY

The primary purpose of this study is twofold. Firstly, unique 2-D and 3-D temperature fields for bare finite rod bundles are presented which result from detailed distributed-parameter analyses using the slug flow model. Secondly, these results together with azimuthally varying inside and outside pressure fields are used to derive thermoelastic stress and displacement fields.

The 2-D temperature fields are obtained by an iterative multicell, multiregion technique. Multicell calculations are especially important for studying the pronounced asymmetry effects induced by the coolant cells which are bounded by the bundle wall. The solution takes into account an arbitrary flow split between wall and internal subchannels as well as different heat source densities in the pins. Results indicate that the adiabatic single cell calculation is not conservative under all circumstances as has been previously assumed. Integral mixing transport parameters which account for local temperature variations are quite different from those which are built into the subchannel codes and should be preferred in the future. The pin model used in these studies incorporates the following features:

— tilted power distribution as experienced across blanket rods,
— eccentric pellet position as the most probable pellet location at BOL,
— cracked pellet under higher burnup conditions.

For the first time, these internal pin disturbances are taken into account together with the external disturbances induced by coolant channel asymmetrics. Hot-spot midwall temperatures are shown. Under low flow conditions additional free convention effects come into effect. The fully-developed mixed convection problem is analytically solved for all types of cells in finite bundles. The clad region is fully integrated in this solution, too. The parametric effect of the Ra-number on velocity and temperature fields are shown and a criterion is presented which indicates the onset of local flow reversal.

Due to the fact that LMFBR cores are quite short, thermal entrance effects may play an important role. A 3-D analysis confirms this and shows that thermal conduction predominates in this regime. A comparison with recent liquid-metal cooled 19-pin bundle experiments shows excellent agreement. Mixing parameters which account for the thermal entrance effect are presented. The broad spectrum of local temperature results indicates that 2-D or even 3-D analyses are required to reveal the highest clad midwall temperature which governs the swelling behavior of LMFBR-fuel pin clads. Hitherto used subchannel codes cannot provide this detailed information and should be extended such, as to incorporate a local model in the region of interest.

1. INTRODUCTION

Recent developments of computer codes for the thermal-hydraulic [1] and structural [2] analysis of LMFBR rods indicate a growing need for multidimensional analysis. Seemingly, it has been fully recognized by now that at least two dimensional (r,ϕ) and (r,z) analyses are absolutely necessary in order to cope with the thermal and structural design constraints of todate's LMFBR rod designs. Actually, 3-D, distributed parameter analyses for fuel, clad, and coolant temperature fields are needed for the reliable design of LMFBR fuel, blanket and absorber assemblies rods to provide the necessary information to accurately evaluate the respective cladding strains which effectively determine the allowable burnup and thus the lifetime of these assemblies. Specifically, the following features should be included in such analyses all of which induce asymmetrical fuel and clad temperature fields.

1. capability to assess the effect of variations in coolant channel geometries specifically those which characterize assembly wall near regions.
2. capability to account for changes in the convective heat transport mode as for instance transition from turbulent to laminar flow heat transfer with and without natural convection effects.
3. capability to assess the effects of power gradients across the rod
4. possibility to account for pellet/cladding eccentricity and ovality as well as pellet cracking.

Certainly, these four disturbances lead to more or less localized increases in the cladding temperatures and cladding strain and hence may increase the clad life damage and thus possibly reduce the allowable burnup and lifetime of the respective assemblies. Furthermore, circumferential gradients support the rod bowing process by a structural-thermal-hydraulic feedback effect and thus lead to an undesirably high mechanical rod-grid (wire spacer) interaction with resultant grid (wire spacer) assembly wall interactions.

Although the individual contributors enlisted above have long been recognized, their effects upon the cladding temperature have been studied only under various simplifying assumptions thus far. Most of these studies [3,4,5] thermally decoupled the heat transport between rod and coolant by using the concept of the heat transfer coefficient. Thus, the superior circumferential heat transport in the coolant has never been taken into account in the past. On the other hand, these procedures disregarded the additional disturbance induced by the asymmetrical coolant channel geometry. Thus, it is not clear whether the results of these former studies constitute a conservative or non conservative basis. The only way to find out is to treat all disturbances simultaneously as the present study does because it is thought that under certain circumstances the combined effect of variations in the source, sink and boundary conditions may lead to an amplification of circumferential cladding temperature variations.

Todate's design methods for evaluating rod temperatures heavily rely upon the use of lumped-parameter subchannel codes such as COBRA-III C [6] and the

like, which determine the bulk coolant temperatures in the subchannels across an assembly as function of the axial location. The temperature of the hottest subchannel around a rod is used then to perform a one-dimensional radial heat transport analysis through the rod by employing the concept of the heat transfer coefficient to derive the cladding temperature. Recently, some methods emerged which take the different bulk temperatures of the subchannels surrounding the rod of interest and employ those as boundary conditions in a two-dimensional thermal analysis of the rod by assuming a constant heat transfer coefficient between the cladding and the coolant. It is worth mentioning that this procedure in even a more advanced form has been already been applied in 1971 [7]. Naturally, although a step forward as compared to the one-dimensional analysis, this remains quite a crude approximation because as already shown by various authors in the past the concept of the heat transfer coefficient breaks down in cases where the defining variables are themselves strong functions of the independent variables. Exactly this has to be expected however in assemblies with very tight pitch-to-diameter ratios such as blanket and absorber assemblies. Yet, due to the lack of more detailed information the aforementioned procedure seems to be the only choice to use the data supplied by subchannel codes right now. Additional insight can only be gained from distributed parameter methods. Due to their complexity the application of these methods have to be restricted to a limiting number of coolant cells surrounding the rod of interest. Thus, in order to obtain meaningful results in the framework of an assembly analysis future efforts should be devoted to develop symbiotic hybrid methods for combined lumped and distributed parameter analysis. A step towards this goal has been undertaken in the present study by interpreting the free unknown in the analytical solution in terms of the bulk temperature which can be supplied by subchannel codes for different axial locations.

Besides of providing directly deterministic local peak temperatures which can be fed into todate's probabilistic design tools for checking the calculated values against the design limits, the distributed parameter methods can be used to generate more reliable integral parameters for updating the effective mixing coefficients for the various transport phenomena incorporated into the subchannel codes. Thus far, only limited informations are available mainly for coolant regions inside an assemblies. However, nothing is known for coolant regions close to the assembly wall, despite the fact that the latter are of more importance for the thermal analysis due to the strong geometrical asymmetries in these regions. The present study will present effective conduction mixing lengths for the corner cells of hexagonal bundles.

Thus far, two-dimensional temperature fields have been mostly used in connection with thermalelastic cladding analyses [3,7,8]. A recent study [9] of clad ovalities as found during post-irradiation examination confirmed that this is not necessarily a bad choice in the first place. At least, deformations agreed very well with the experimental evidence although the

calculated stresses turned out to be twice the yield strength. Because thermoclastic analysis is the first logical choice entering the structural field it was decided to work with the codes described in [3,7] to determine the radial and tangential displacements. Due to the fact that the thermoelastic strains alone are unrealistically high the GRO-II code [10] is used to perform an order of magnitude analysis for the nonlinear effects. For this purpose the highest cladding midwall temperature as determined by the 2-D or 3-D thermal analysis has been used as input into this one-dimensional structural analysis code. Finally, this present study uses the two-dimensional nonlinear structural analysis code GOGO [2] to check the approximate results obtained by GRO-II and to obtain more detailed results for the local phenomena. GOGO is the only 2-D code in r-ϕ geometry known to the authors which handles all nonlinear effects relevant to LMFBR operational conditions within an affordable amount of computational efforts. It is worth mentioning that the original version of this code contained a very crude approximation of the clad temperature variation of a corner pin which has been changed for the present analysis according to the newly derived analytical results. Due to the limited space available only highlights of the basic findings of the whole study can be reproduced in the following figures. More details will be disclosed during the presentation and in follow-on publications [11,12].

2. ANALYSIS

2.1. Thermal Analysis

In what follows, short descriptions will be given about the underlying principles for two 2-D and one 3-D thermal-hydraulic analyses in typical subsections of hexagonal LMFBR assemblies.

2.11 2-D Multicell, Multiregion Slug Flow Heat Transfer Analysis

Thus far, only single cell, multiregion analyses have been reported for coolant regions close to the assembly wall [13] (see Fig. 1), although some progress has been made in the past to couple several internal cells in two [1] and three dimensions. However, despite of the value of the basic findings in this geometry the more interesting regions with respect to design are the outer coolant cells such as the corner cells (see Fig. 1) and the side cells. Multicell analyses are necessary in order to avoid the adiabatic boundary conditions around the polygonal sides of the coolant cells to study the propagation of disturbances across cell boundaries either from inside the bundle due to power skews and/or outer regions due to assembly wall effects. In order to perform efficiently a multicell analysis for a rod bundle or sections thereof it is essential to develop a scheme which can uniquely identify any individual unit cell as a function of the cell number. For this purpose, a double index system (m,n) has been developed [14], where the first index indicates the number of rows from the center of the bundle and the second one designates the distance between the cell center and the normal to the bundle wall in terms of number of pitches. By virtue of this system each cell and more important the types of its neighbors can be automatically identified.

The present study adopts the slug flow heat transfer as an approximation to turbulent liquid-metal heat transfer. The multiregion temperature solutions for fuel, clad and coolant are derived for all types of cells in a finite bundle under the assumption of adiabatic conditions around the cell boundaries. For this purpose the solutions presented in [13] have been adopted. Naturally the separate adiabatic calculations of different cells result in temperature discontinuity along the imaginary matching boundary in the coolant between the two cells. An iterative method has been developed [12] which removes systematically this temperature difference by imposing the condition of heat flux continuity along the same line. The scheme can be explained for the geometry shown in Fig. 1 as follows. For the coolant temperature field of cell i - the corner cell - the adiabatic solution reads

$$T_i^{(o)}(\rho,\phi) = A_i + \frac{q_i''' a^2}{2k_3} \theta_j(\rho,\phi) \quad , \tag{1}$$

whereas for cell j - the internal cell - the coolant temperature is represented by

$$T_j^{(o)}(\rho,\phi) = A_j + \frac{q_j''' a^2}{2k_3} \theta_j(\rho,\phi) \tag{2}$$

The superscript o denotes the zeroth iteration. Starting with these initial solutions an updated coolant temperature field for the corner cell can be derived which is followed then by a calculation of an updated heat flux distribution along the common boundary. This is used as boundary condition for the neighboring cell which in turn leads to a new temperature field. The second iteration starts with the updated temperature boundary condition and so forth. In order to relate the outcome of this study to the results of subchannel codes a unique relationship for the differences of the average coolant cell temperatures has been established. This difference together with the evaluation of the heat transferred across the common cell boundary yields the effective conduction mixing length scale, l_{ij}, which is employed in subchannel codes. l_{ij} is given by

$$l_{ij} = k \frac{S_{ij}(\bar{T}_i - \bar{T}_j)}{\int_{S_{ij}} q''_i \, ds} \tag{3}$$

For practical purposes, l_{ij} is usually set equal to the centroid-to-centroid distance between subchannels, l_{ij}^*, i.e.,

$$l_{ij} = l_{ij}^* \quad . \tag{4}$$

However, this assumption is not valid at all. Therefore, the present study evaluates a correction factor, L_{ij}, given by

$$L_{ij} = \frac{l_{ij}}{l_{ij}^*} = k \frac{S_{ij}}{l_{ij}^*} \frac{(\bar{T}_i - \bar{T}_j)}{\int_{S_{ij}} q''_i \, ds} \qquad (5)$$

where S_{ij}/l_{ij}^* can be simply expressed in terms of geometrical parameters alone as

$$\frac{S_{ij}}{l_{ij}^*} = \frac{\frac{1}{2}\left(\frac{P}{D}-1\right)}{\left[\frac{\frac{1}{16}\left(\frac{2W}{P}\right)^2\left(\frac{P}{D}\right)+\frac{1}{24\sqrt{3}}\left(\frac{2W}{D}\right)^3-\frac{1}{16}\quad\frac{1}{2}\left(\frac{P}{D}\right)^3-\frac{\sqrt{3}}{12}\pi\left(\frac{P}{D}\right)}{-\frac{1}{4}\left(\frac{P}{D}\right)\left(\frac{2W}{D}\right)+\frac{1}{8\sqrt{3}}\left(\frac{2W}{D}\right)^2-\frac{1}{12}\pi} + \frac{}{\sqrt{3}\left(\frac{P}{D}\right)^2-\frac{1}{2}\pi}\right]} \qquad (6)$$

By virtue of the above procedure distributed parameter methods can provide meaningful informations for use in today's design codes and thus may help to improve the reliability of their results in cases where a priori no experimental evidence is available for tuning purposes.

In order to account for the additional effects of pellet eccentricity and cladding ovality the analytical formulation presented in [3] has been iteratively tied together with the present analysis.

2.12 3-D Single and Multicell, Single Region Slug Flow Heat Transfer Analysis

The analysis presented in the preceding section assumes thermally fully-developed conditions. Due to the high asymmetry effects induced by the corner and side cells and the relatively small core heights it may be argued that this assumption is invalid in reality. In order to check this a three-dimensional slug flow heat transfer analysis has been conducted on the basis of the analysis performed in [15]. The overall solution can be split into a fully developed part and an entrance solution part. The latter is given in general information form as

$$\theta_e(\rho,\phi,\xi) = \sum_{n=o}^{\infty}\sum_{m=1}^{\infty}\left[C_{n,m}J_n(\beta_m\rho)+D_{n,m}Y_n(\beta_n\rho)\right] E_m e^{-\beta_m^2\xi}\cos n\phi \qquad (7)$$

The assumption of slug flow under these circumstances seems to be quite justified because heat conduction constitutes a major part of the overall heat transport for liquid-metal flow in the entrance region especially for low and moderate flow conditions. Whereas the analysis in [15] was limited to a single cell, the present study extended the analytical procedure to analyze the coupled behavior of two cells as shown in Fig. 1. Due to the vastly different entrance region behavior of internal and corner cells special attention had to be devoted to minimize the numerical interior and boundary least square

errors introduced at the inlet section by satisfying the boundary condition of constant temperature over the total inlet cross-sectional area. Due to the fact that this analytical analysis is solely confined to the coolant region the assumption of constant heat flux around the outer cladding surface has been introduced. This simplification leads to conservative results for the circumferential cladding temperature variation due to the neglection of the azimuthal heat conduction effects in the cladding. Arbitrarily varying heat flux distributions in the axial direction are handled by Duhamel's superposition principle.

2.13 Fully-Developed, Single Cell, Two-Region Analysis of Laminar Mixed Convection Heat Transfer

Under low flow conditions as experienced in recent blanket assembly designs or in case of loss-of-flow in either fuel and/or blanket assemblies the assumption of turbulent flow and hence the slug flow approximation is certainly invalidated. The transition to laminar flow is accompanied by a substantial deterioration of the heat transfer from the rod to the coolant which may lead to an even higher circumferential cladding temperature variation. Therefore, the designer is very much interested to find out whether a superimposed natural convection effect may help to avoid the very low heat transfer regime. In order to study the mixed convection capabilities of typical unit cells in finite, hexagonal bundles with respect to local as well as average quantities a two-region analysis has been performed [16]. The general solutions for the temperature fields in the coolant and cladding assume the following forms, respectively

$$t_{c0}(r,\phi) = -\frac{1}{\eta^4} + \frac{1}{\eta^2}\sum_{n=0}^{\infty}\left[a_{sn}\,bei_{sn}(\eta r) - b_{sn}\,ber_{sn}(\eta r) + c_{sn}\,kei_{sn}(\eta r) - d_{sn}\,ker_{sn}(\eta r)\right]\cos(sn\,\phi) \tag{8}$$

$$t_{c1}(r,\phi) = A_o - \frac{\bar{q}''H}{k_3}\,a\,\ell n\,r + \left[A_1 + \frac{a^2}{r^2}\,(A_1 - \frac{\bar{q}''F}{k_3})\right]r\cos\phi + \sum_{n=2}^{\infty} r^n\left[1 + (\frac{a}{r})^2\right]A_n\cos(n\,\phi) \tag{9}$$

The coefficients in these equations are found by simultaneously solving these equations together with the general solution for the velocity field when substituted into the various boundary conditions. It is worth mentioning that Eq. (9) accounts for an azimuthally varying heat flux distribution at the cladding inside surface, thus simulating a power tilt across the fueled region.

2.2 Thermoelastic and Inelastic Analyses

The thermoelastic analyses are performed by using the methods in [3] and [8]. The former incorporates the possibility to account simultaneously for either pellet eccentricity or cladding ovality together with a superimposed

power tilt across the fueled region whereas the latter one performes a Fourier series analysis of the inside and outside cladding temperatures which have to be supplied as input. The majority of the inelastic studies is performed using the GRO-II code [10] which uses the thin shell approximation. The GOGO-code [2] is used to provide two-dimensional inelastic informations.

3. RESULTS AND DISCUSSION

Most results are obtained for a typical average corner pin of a fuel assembly and a peak corner pin of a blanket assembly for the CRBPR. Figure 2 shows the effect of a typical power tilt across the assembly upon the cladding temperature variation of the corner pin. Under the given circumstances the least variation can be expected when the tilt is decreasing towards the assembly center. Figure 3 demonstrates the quite different temperature variations in the individual unit cells as derived by a four-cell calculation. It is interesting to notice that the cladding temperature variation of cells 2 and 3 are about the same although both represent different locations within the assembly. Figure 4 represents the correction factor L_{ij} as function of the dimensionless wall distance for a given P/D. Obviously, L_{ij} deviates quite substantially from 1 which means that the common assumption of using the centroid-to-centroid distance as effective conduction mixing length is incorrect. Under extreme conditions the direction of the heat flow is even reversed. Figure 5 comprises a comparison between the 3-D slug flow heat transfer analysis and experimental evidence [17] as measured in a sodium cooled 19-rod bundle. Despite the stringent assumptions built into the analysis the agreement can be considered as quite satisfactory. In order to show the effect of coupling two different cells together, Fig. 6 compares the results of a single cell to a two-cell calculation. The "bump" in the cladding temperature which shows up at about 120 degrees can be attributed to the additional heat flow out of the internal cell into the corner cell. Overall, the comparison to two-dimensional calculations show that these overpredict the cladding temperature variations by about a factor of two. Thus, the 3-D calculations are necessary and meaningful to derive a scaling factor in order to realistically apply the 2-D results presented before. Figures 7 through 9 summarize some of the findings of the mixed convection study. It is obvious that for higher Ra-numbers the velocity field gets highly distorted and that locally coolant regions with downflow exist. Naturally, this affects both local and average thermal quantities as shown in Figs. 8 and 9. It is interesting to notice that $\overline{Nu}$ after increasing over a certain Ra-number range rapidly decreases beyond a certain critical Ra-number and assumes values which are lower than those for laminar convection only. As indicated these effects are strongly dependent upon the cell geometry.

Figures 11 through 13 summarize the results of the two-dimensional thermo-elastic analysis whereas Figs. 14 and 15 depict the results of the one-dimensional inelastic analysis using the GRO-II code. The temperature

distributions which were used as input are shown in Fig. 10 for the fuel and the blanket assembly. The blanket rod experiences about twice the radial displacement of the fuel rod. The circumferential variation is largest for large wall distance and in case that the power tilt is directed towards the assembly wall. Overall, these results suggest that the corner rod moves towards the interior rod and hence reduces the coolant areas in a regime which is already characterized by higher temperatures. Thus, this feedback effect will lead to even higher temperatures at 180 degrees. The least variation is experienced in case that the wall distance is slightly less than P/D = 1.08. Here the rod closes the gap towards the side pin. The circumferential variation of u is substantially lower for the fuel rod. The largest variation in the tangential displacement occur for the large wall distance design as shown in Fig. 12. The maximum of v is located at an angular position between 110 and 120 degrees. Figure 13 demonstrates that the variation of the tangential stress distributions of all cases considered for the blanket rod are bounded by the two cases studied for the fuel rod.

Figures 14 and 15 show the effects of different temperature levels upon the total creep in blanket and fuel rods. Due to the simple approach incorporated in GRO-II it has been assumed that the rods are characterized either by an average temperature or by the maximum midwall temperature found by the aforementioned 2-D thermal analysis. As can be seen from the figure, the creep is about an order of magnitude higher for the maximum temperature than for the average one. The circumferential variation of the cladding creep is approximately bounded by the two lines given in the figure. Obviously this variation increases with burnup. This increase might be even larger because the minimum cladding temperature stays below the average one. As Fig. 15 depicts the fuel rod shows a similar behavior over most of its burnup in case of 20% CW 316 SS as cladding material. There again the high temperature region of the cladding circumference will creep more by an order of magnitude than the cooler parts. However, starting halfway through lifetime of the fuel the overall circumferential variation in creep behavior decreases and from 8% burnup on the fuel rod cladding nearly creeps in a uniform fashion. Annealed 316 SS behaves quite differently. There the cooler parts creeps more than the hotter ones and the difference keeps obviously growing with burnup. From an overall design point of view this might be a desirable feature. Naturally, the reported results heavily rely upon the correlations for the material properties built into GRO-II.

ACKNOWLEDGEMENTS

The authors appreciate the financial support for this study by the U.S. ERDA.

REFERENCES

[1] CHUANG, M.C., "Cladding Circumferential Hot Spot Factors for Fuel and Blanket Rods," Nucl. Eng. Design 35, 21 (1975).

[2] SIM, R.G., GOGO User's Manual," GEAP-13968 (1973).

[3] WOLF, L., "Thermo-Elastic Stresses in Fuel Element Clads Due to the Combined Effects of Flux Tilt in the Fuel and Circumferential Variations of Boundary Conditions," Proc. 2nd Int. Conf. SMIRT, Berlin, Germany (September 10-14, 1973), Paper C314.

[4] NIJSING, R., "Temperature and Heat Flux Distribution in Nuclear Fuel Element Rods," Nucl. Eng. Design, 4, 1 (1966).

[5] GODESAR, R., "Influence of Azimuthal Perturbation of Heat Transfer in the Gap on Design and Irradiation Behaviour of Fuel Pins," Proc. Int. Conf. Physical Metallurgy of Reactor Fuel Elements, CEGB, 1973, 308-314

[6] ROWE, D.S., "COBRA-IIIC: A Digital Computer Program for Steady State and Transient Thermal-Hydraulic Analysis of Rod Bundle Nuclear Fuel Elements," BNWL-1695 (May 1973).

[7] FISCHER, M., HOFMANN, F., KRIEG, R., "Mechanical Loads of Claddings by Azimuthal Temperature Gradients in Fuel Pins with Eccentric Geometry," (in German), Proc. 1st Int. Conf. SMIRT, Berlin, Germany, September 20-24, 1971, Paper C212.

[8] CROZIER, R.J.M., "SEGPIPE: A Program to Determine Thermo-Elastic Deformations in a Segment of a Hollow Cylinder," AECL-4056 (1971).

[9] KERRISK, J.F., BARNER, J.O., PETTY, "Cladding Ovalities in Advanced Liquid-Metal Fast Breeder Reactor Fuel Elements," Nucl. Technology 30, 361 (1976).

[10] PATEL, M., WHITE, D.E., "GRO-II: A Simplified Method for Predicting Mixed Oxide Fuel Rod Performance During Normal Operation," GEAP-14051 (1975).

[11] KARIMI, R., "Two-Dimensional Inelastic Cladding Loading Sensitivity Analyses," M.S. Thesis, Dept. Nucl. Engng., MIT, to be published

[12] YEUNG, M., "Multicell Fluid Flow and Heat Transfer Analysis in Rod Bundles," Ph.D. Thesis, Dept. Nucl. Engng, MIT, to be published.

[13] WOLF, L., JOHANNSEN, K., "Two-Dimensional, Multiregion Analysis of Temperature Fields in Finite Rod Bundles Cooled by Liquid Metals," Proc. 1st Int. Conf. SMIRT, Berlin, Germany, September 20-24, 1971.

[14] Progress Report: "Coolant Mixing in LMFBR Rod Bundles and Outlet Plenum Mixing Transients," Dept. Nucl. Engng., MIT COO-2245-31 (1976).

[15] MEIER, S., "An Analytical Solution for the Temperature Fields in Liquid-Metal Cooled Fuel Pin Bundles with Arbitrary Axial Heat Flux Profile," (in German) Ph.D. Thesis, Institut für Kerntechnik, Berlin, Germany, TUBIK-37, 1974.

[16] KIM, J.Y., "Fully-Developed Mixed Convection Heat Transfer in Finite Hexagonal Bundles," M.S. Thesis, Dept. Nucl. Engng., MIT (Feb. 1977).

[17] MÖLLER, R., TSCHÖKE, H., "Experimental Determination of Temperature Fields in Sodium-Cooled Pin Bundles," (in German), Nucl. Conf., Düsseldorf, Germany, 1976.

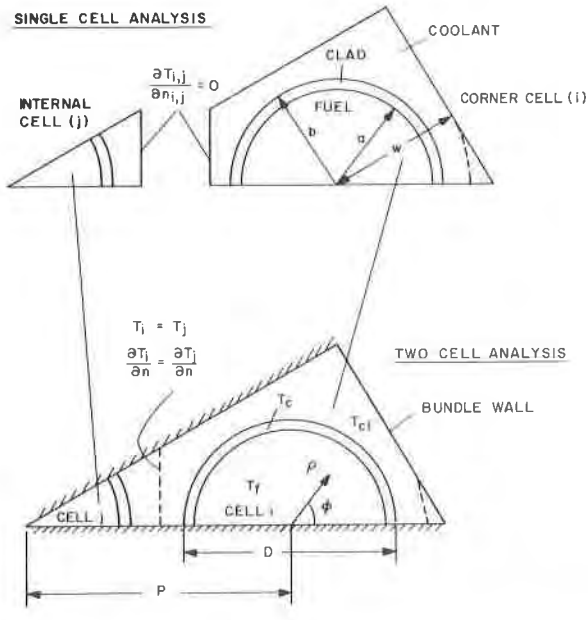

Fig. 1 Single Cell and Two Cell Geometries.

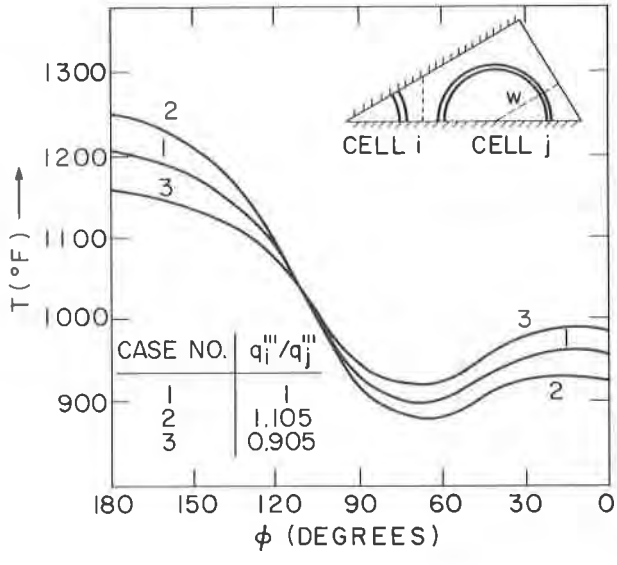

Fig. 2 Effect of Different Power Generation Rates in Adjacent Fuel Pins of the Radial Blanket Upon Outside Clad Temperature Distribution of the Corner Pin ($\bar{T}_{clad}$ = 1000°F)

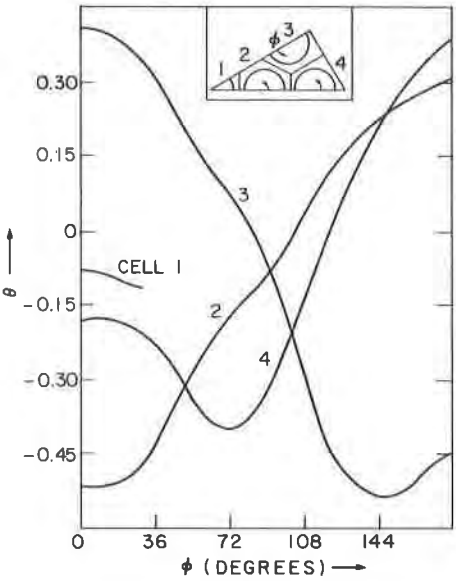

Fig. 3 Dimensionless Outside Clad Temperature Distributions as Calculated by a Four-Cell Analysis (P/D = 1.205; 2W/D = 1.2)

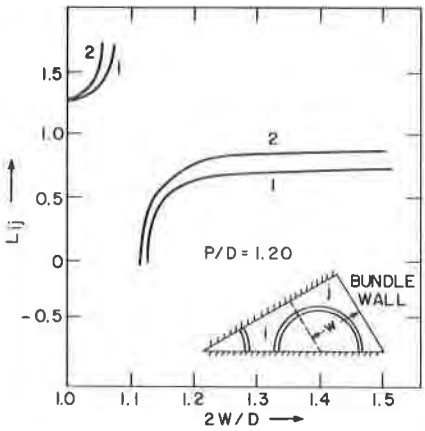

Fig. 4 Dimensionless Effective Conduction Mixing Length L_{ij} as Function of 2W/D for: 1) Azimuthally Uniform Heat Flux at Outside Clad Surface
2) Multiregion Analysis

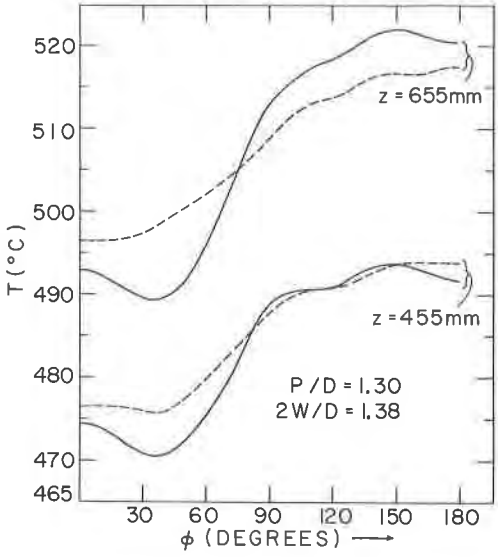

Fig. 5 Comparison between Experiment [17] (---) and Single-Cell, 3-D Analysis (—) for the Outside Clad Temperature Distribution of a Side Pin

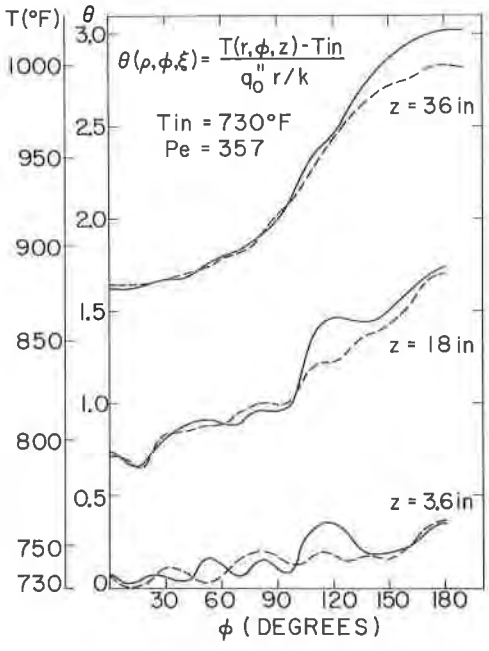

Fig. 6 Comparison of Outside Clad Temperatures for a Corner Pin in a Fuel Assembly as Obtained from Single-Cell,3-D (---) and Two-Cell (—) Analyses

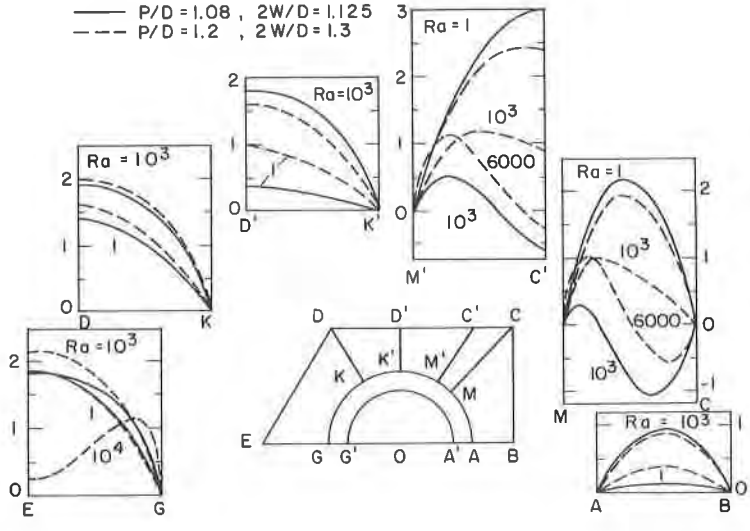

Fig. 7 Effect of Mixed Convection Upon the Velocity Profiles in a Side Cell for Two Different Designs

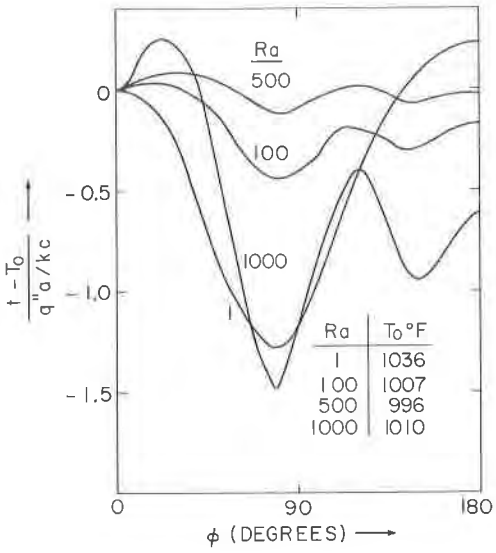

Fig. 8 Effect of Different Ra-Numbers Upon the Corner Pin Cladding Temperature Distribution of a Blanket Assembly ($q' = 1$ KW/ft, $\bar{T}_{co} = 995°F$, $T_o = T_c(b,0)$)

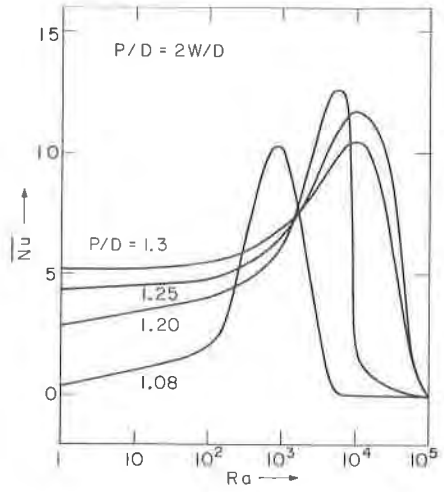

Fig. 9 Average Nusselt Number for the Side Cell as Function of Ra ($P_{wet} = \pi\ b + P/2$)

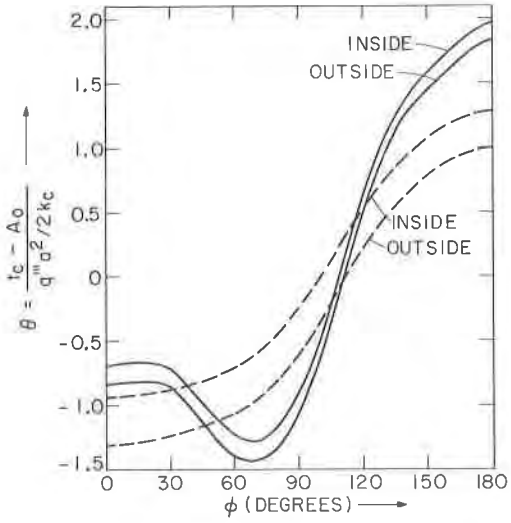

Fig. 10 Dimensionless Inside and Outside Caldding Temperature Distributions for Fuel (---) and Blanket (⟷) Assembly Corner Rods as Derived from Fully-Developed Slug Flow Analysis

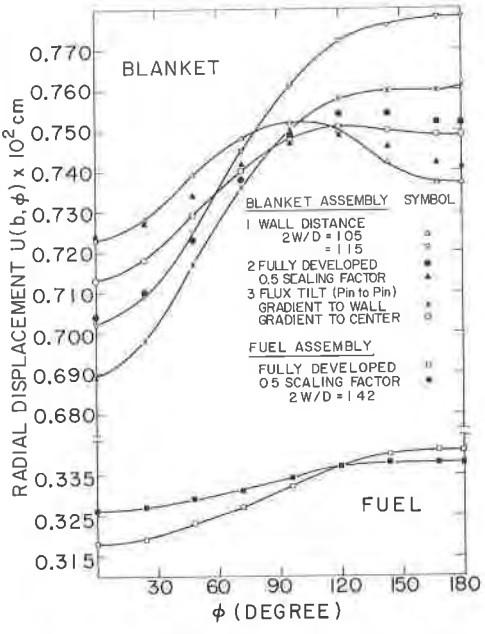

Fig. 11 Thermoelastic Circumferential Radial Displacement of the Outer Cladding Surface for Different Assumptions and Conditions

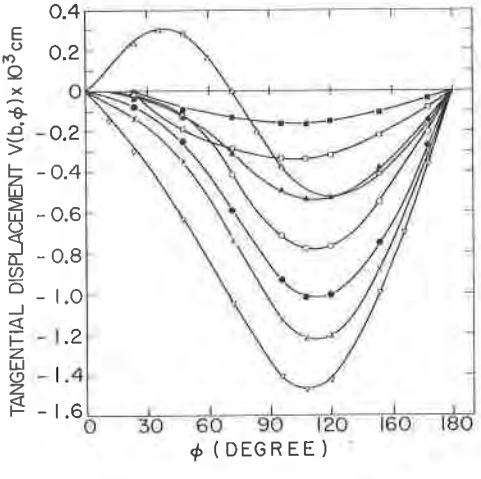

Fig. 12 Azimuthal Variation of Thermoelastic Tangential Displacements of the Outside Cladding Surface (For Symbols see Insert in Fig. 10)

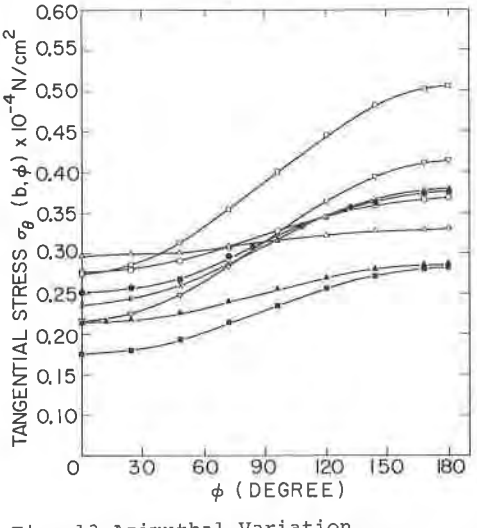

Fig. 13 Azimuthal Variation of Thermoelastic Stress Distributions (for Symbols see Insert in Fig. 10)

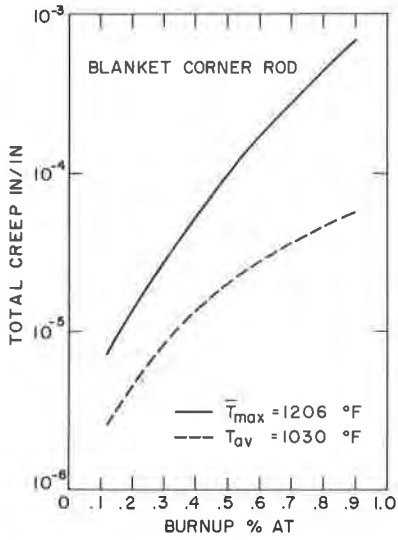

Fig. 14 Total Clad Creep (Thermal, Irradiation, Swelling) as Function of Burnup for a Blanket Corner Rod with Average and Maximum Temperature Loads (Material: 20% CW 316 SS)

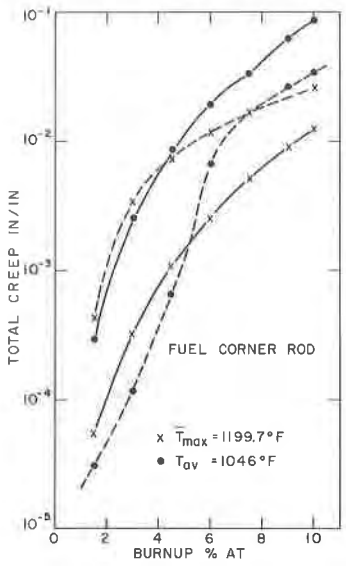

Fig. 15 Total Clad Creep (Thermal, Irradiation, Swelling) as Function of Burnup for a Fuel Corner Rod with Average and Maximum Temperatue Loads (— Annealed 316 SS; --- 20% CW 316 SS)